Hydrol. Earth Syst. Sci. Discuss., 10, 12453–12483, 2013
www.hydrol-earth-syst-sci-discuss.net/10/12453/2013/
doi:10.5194/hessd-10-12453-2013

Hydrology and Earth System Sciences
Open Access
Discussions

Forecasting terrestrial water storage changes in the Amazon Basin using Atlantic and Pacific sea surface temperatures

C. de Linage[1], **J. S. Famiglietti**[1,2], **and J. T. Randerson**[1]

[1]Department of Earth System Science, University of California, Irvine, USA
[2]UC Center for Hydrological Modeling, University of California, Irvine, USA

Received: 25 September 2013 – Accepted: 30 September 2013 – Published: 15 October 2013

Correspondence to: C. de Linage (caroline.delinage@uci.edu)

Published by Copernicus Publications on behalf of the European Geosciences Union.

Abstract

Floods and droughts frequently affect the Amazon River basin, impacting transportation, river navigation, agriculture, and ecosystem processes within several South American countries. Here we examined how sea surface temperatures (SSTs) influence interannual variability of terrestrial water storage anomalies (TWSAs) in different regions within the Amazon basin and propose a modeling framework for inter-seasonal flood and drought forecasting. Three simple statistical models forced by a linear combination of lagged spatial averages of central Pacific (Niño 4 index) and tropical North Atlantic (TNAI index) SSTs were calibrated against a decade-long record of 3°, monthly TWSAs observed by the Gravity Recovery And Climate Experiment (GRACE) satellite mission. Niño 4 was the primary external forcing in the northeastern region of the Amazon basin whereas TNAI was dominant in central and western regions. A combined model using the two indices improved the fit significantly ($p < 0.05$) for at least 64 % of the grid cells within the basin, compared to models forced solely with Niño 4 or TNAI. The combined model explained 66 % of the observed variance in the northeastern region, 39 % in the central and western regions, and 43 % for the Amazon basin as a whole with a 3 month lead time between the SST indices and TWSAs. Model performance varied seasonally: it was higher than average during the rainfall wet season in the northeastern Amazon and during the dry season in the central and western regions. The predictive capability of the combined model was degraded with increasing lead times. Degradation was smaller in the northeastern Amazon (where 49 % of the variance was explained using an 8 month lead time vs. 69 % for a 1 month lead time) compared to the central and western Amazon (where 22 % of the variance was explained at 8 months vs. 43 % at 1 month). These relationships may enable the development of an early warning system for flood and drought risk. This work also strengthens our understanding of the mechanisms regulating interannual variability in Amazon fires, as water storage deficits may subsequently lead to decreases in transpiration and atmospheric water vapor that cause more severe fire weather.

HESSD

10, 12453–12483, 2013

1 Introduction

The Amazon River basin has experienced several severe droughts during the last decade (Marengo et al., 2008, 2011; Chen et al., 2009; Espinoza et al., 2011; Lewis et al., 2011; Frappart et al., 2012), with extreme events in 2005 and 2010 increasing forest mortality (Phillips et al., 2009; Lewis et al., 2011) and the number of satellite-detected fires (Chen et al., 2013b). More frequent extreme wet events also have been observed in the Amazon in the last 20 yr (Chen et al., 2010; Boening et al., 2012; Espinoza et al., 2013; Gloor et al., 2013). Droughts and floods lead to important economic losses by affecting land and river transportation, agriculture, fisheries (Drapeau et al., 2011) and hydropower generation (Lima and Lall, 2010). They also influence seasonal and interannual variability of the regional carbon budget by modifying photosynthesis, tree mortality, fires, rates of autotrophic and heterotrophic respiration, and river dissolved organic carbon fluxes (e.g. Richey et al., 2002; Baker et al., 2008; Phillips et al., 2009; Lewis et al., 2011; Miller et al., 2011; Davidson et al., 2012). Such extreme events may become more frequent in a changing climate due to increased precipitation extremes (Kitoh et al., 2013). To limit economic and ecosystem impacts, an important goal is to provide managers with early warning information about drought and flood risk based on observations of key climate system predictors.

While the influence of the El-Niño Southern Oscillation on the Amazon's hydroclimatology is well established (e.g. Ropelewski and Halpert, 1987; Richey et al., 1989; Enfield, 1996; Zeng, 1999; Dettinger et al., 2000; Liebmann and Marengo, 2001; Ronchail et al., 2002; Dai et al., 2009; Molinier et al., 2009; Lima and Lall, 2010; van der Ent and Savenije, 2013), several recent studies have identified ocean–atmosphere coupling in the tropical Atlantic as another key regulator of hydrological variability within the basin (Zeng et al., 2008; Molinier et al., 2009; Yoon and Zeng, 2010; Espinoza et al., 2011). These latter studies provide evidence that an anomalous northward shift of the position of the intertropical convergence zone (ITCZ) contributed to the severe 2005 and 2010 droughts in the central and western Amazon. Therefore, a dual external forcing

HESSD
10, 12453–12483, 2013

seems to control the Amazon's hydrology and climate on interannual time scales. Evidence for this also comes from ecological studies that show both equatorial Pacific and North Atlantic sea surface temperatures (SSTs) are correlated with many variables that influence terrestrial ecosystem drought stress, including precipitation, evapotranspiration, surface relative humidity, and the number of satellite-detected active fires (Chen et al., 2011, 2013a). These variables, while crucial for assessing climate impacts on terrestrial ecosystem function, are not direct indicators of variations in regional water budgets. Specifically, precipitation is only one of several variables contributing to the surface water mass balance of soils and aquifers, and fires occur as a consequence of a complex set of feedbacks between humans, ecosystem processes and climate. Additional information is needed to understand more directly how tropical climate modes influence regional variations in terrestrial water storage within the Amazon basin.

Here we analyzed the relationship between SSTs and anomalies of vertically integrated terrestrial water storage (TWSAs) derived from NASA's Gravity Recovery And Climate Experiment (GRACE) mission. GRACE satellite observations have been used along with precipitation data to predict floods worldwide with a one-month lead time, by estimating the saturation level of the land surface (Reager and Famiglietti, 2009). In the Amazon basin, statistically significant teleconnections between GRACE TWSAs and either Pacific or Atlantic SSTs were identified by de Linage et al. (2013), suggesting that SSTs may be used as a proxy for the balance between precipitation and evapotranspiration.

We build on this work in the current study by developing a series of statistical models that are driven by SSTs and used to explain variability in terrestrial water storage across different river basins and regions within South America. These models are forced by Pacific or Atlantic SSTs with variable lead times relative to the TWSA time series (nominally 3 months but varying between 1 and 8 months). In the data section we describe the source and processing steps used to prepare the GRACE and SST observations used in our analysis. In the methods section we discuss how we developed our statistical models, including calibration and evaluation approaches. In the results section,

HESSD
10, 12453–12483, 2013

we show how the relative importance of tropical Pacific and Atlantic SSTs vary across different regions within the Amazon in terms of their controls on temporal variability of TWSAs, the degree to which forecast model predictions are improved when information from Pacific and Atlantic SSTs are used together, and seasonal variations in model forecasting skill. Because of the potential to use our statistical models for drought and flood risk assessment, we also evaluated how model predictive skill was degraded with increasing lead times.

2 Data

Our study domain encompassed the Amazon River basin and several neighboring regions: the Araguaia-Tocantins River basin to the east, the Maroni, Courantyne and Essequibo River basins to the northeast, the Orinoco River basin to the north, the Magdalena River basin to the northwest, the coastal and mountainous areas of Ecuador and Peru to the west and the Titicaca and Poopó Lakes' System to the southwest (Fig. 1).

2.1 GRACE terrestrial water storage anomalies

We used the GRACE-Release 2 solutions computed by the Groupe de Recherche en Géodésie (GRGS) (Bruinsma et al., 2010). They consist of water storage anomalies expressed in equivalent water height, that are the sum of surface water, snow, soil moisture and groundwater, at a spatial resolution of 400 km at the equator and with an uncertainty of about 30 mm on average over our study domain (given by the RMS of the GRACE variations over the open-ocean domain within the same latitude range following Chen et al., 2009). TWSAs are the deviations from a reference value during the study period, as absolute levels cannot be measured. No post-processing was performed because the regularization constraint applied in the inversion of the GRACE raw observations aims to reduce the noise without the need of additional filtering tech-

HESSD
10, 12453–12483, 2013

niques (Bruinsma et al., 2010). The 10 day fields were linearly interpolated in the gaps and decimated to a monthly time step for consistency with the SSTs. The available GRACE record spanned the period from August 2002 to July 2012. The TWSAs were computed on a 3° × 3° grid (~ 330 km × 330 km at the equator) from the Stokes coefficients to minimize redundant information and to avoid under-sampling. In each grid cell, the mean monthly climatology of the 10 yr period was subtracted from the data. The residual interannual TWSA amplitudes ranged from −280 to 360 mm over the 112 grid cells and their standard deviation varied between 20 and 135 mm. The largest standard deviation occurred in the northeastern regions including the Rio Branco watershed and the lower Amazon regions downstream of Manaus, the coastal basins of the Essequibo, Maroni and Courantyne Rivers in Guyana, Suriname and French Guyana (Fig. 1). The increase in the dynamical range of storage changes toward the lower Amazon is also found at the annual time scale (de Linage et al., 2013) and can be correlated with an increase in the surface storage capacity due to deeper river beds and higher fractions of inundated area (Prigent et al., 2007).

2.2 Sea surface temperatures

The El Niño Southern Oscillation (ENSO) is a global-scale climate oscillation involving a coupling in the ocean-atmosphere system in the Pacific, with complex teleconnections worldwide. Large-scale subsidence and reduced precipitation over the northeastern regions of tropical South America occur during El Niño, because of a reduction in uplift associated with an eastward shift of the Walker circulation (e.g., Saravanan et al., 2000). Here we used the Niño 4 index from NOAA's Climate Prediction Center (www.esrl.noaa.gov/psd/data/climateindices/list/) as a measure of ENSO influence on South America hydrology (Fig. 2). We chose Niño 4 because in many regions of South America GRACE TWSA time series are correlated more significantly with central Pacific SSTs (represented by the Niño 4 index) than eastern Pacific SSTs (represented by the Niño 3 index) on interannual time scales, as shown by de Linage et al. (2013).

HESSD
10, 12453–12483, 2013

To represent the Atlantic influence on water storage changes in our study domain, we used the Tropical North Atlantic Index (TNAI), also from NOAA's Climate Prediction Center. TNAI is the SST anomaly averaged across the region indicated in Fig. 2 (Enfield, 1999). It is highly correlated ($R^2 = 0.58$, $p < 0.01$) with the Atlantic Multi-decadal Oscillation, that represents SST changes in the whole North Atlantic Ocean and is known to trigger droughts in the US (Enfield et al., 2001; McCabe et al., 2004). TNAI is the oceanic northern component of a meridional sea surface temperature gradient found in the coupled atmosphere–ocean system in the tropical Atlantic Ocean called the Atlantic Meridional Mode. Stronger convergence of surface winds and more rainfall happen in the warmer hemisphere due to a meridional shift of the ITCZ (Enfield, 1996; Chiang and Vimont, 2004). Although the Atlantic Meridional Model is equivalently well correlated to GRACE TWSAs compared to TNAI, we preferred to use TNAI as a predictor because it remains correlated with TWSAs with longer lead times (de Linage et al., 2013). For each climate index, the mean over the GRACE period was subtracted from the data.

3 Methods

3.1 Model description

We considered three linear models in which TWSA is solution of the following first-order differential equation:

$$\frac{\mathrm{dTWSA}(x,t)}{\mathrm{d}t} = -\frac{\mathrm{TWSA}(x,t)}{\tau(x)} + F(t) \quad (1)$$

The first term in the right-hand side of the equation represents the evolution of the system in the absence of external forcing ($F(t) = 0$), i.e. the relaxation from the TWSA initial value to zero with a time constant τ, one of the model parameters. The second term, $F(t)$, represents the forcing (i.e., the impact of the SST anomalies on the

HESSD
10, 12453–12483, 2013

balance between precipitation and evapo-transpiration at each location, x, within the study domain), which prevents the system from returning to a steady state. For the first two models we considered, the forcing consisted in a single climate index (Niño 4 or TNAI), while that of the third model was a linear combination of both indices (Table 1). We assumed the two indices were independent enough to be used simultaneously as predictors. A lead-lag correlation analysis revealed that Niño 4 explained at most 17 % of TNAI's variance ($p < 0.01$) during 1950 to 2012, when Niño 4 led TNAI by 4 months.

Model calibration was done against the 10 yr long time series of monthly GRACE TWSAs. For each model and each parameter set, the solution of the model equation was found numerically using an ordinary differential equation solver, with TWSA(t_0) as the initial condition. Among the different parameter combinations that we tested (Table S1), the one leading to the lowest RMSE was selected. We ensured that the minimum RMSE was reached by investigating large ranges for parameters a_0 and b_0. The range of the relaxation constant τ and that of the predictors' lead times α and β were limited by a priori constraints: an upper limit of 12 months was chosen for τ, while α and β were allowed to vary between 3 and 8 months in our primary set of model analyses presented in Sects. 4.1–4.3. A minimum value of 3 months was chosen to place a reasonable minimum bound on the forecast lead times. Shorter lead times may improve model performance, as investigated in Sect. 4.4, but time delays associated with SST processing and data availability make it unlikely this information could be used effectively in an operational forecasting system. Model 3 (the combined model) used the lead time values that had been optimized for models 1 and 2 (for the individual Niño 4 and TNAI models; Fig. S1) in order to reduce the number of iterations during the parameter optimization.

3.2 Model evaluation

We computed the coefficient of determination R^2 and the normalized RMSE of the linear regression to evaluate model performance. RMSE were normalized by the standard deviation of GRACE TWSAs in each grid cell, shown in Fig. 1. For each model

HESSD
10, 12453–12483, 2013

and in each grid cell, we performed an F test (null hypothesis $F = 0$, $p < 0.05$) to check whether or not the model was statistically better than the temporal mean of the observations. The statistics of the regression are provided in Table 2. Finally, to estimate whether the bivariate (combined) model (forced by Niño 4 and TNAI) was significantly better than each of the two univariate models (forced either by Niño 4 or TNAI), we used another F test (null hypothesis $F = 0$, $p < 0.05$) on the residual sum of squares difference, accounting for the difference in the models' degrees of freedom (given in Table 1).

4 Results

4.1 Spatial patterns of SST controls on terrestrial water storage anomalies

The influence of Niño 4 and TNAI on terrestrial water storage interannual variability varied considerably across different regions in tropical South America (Fig. 3). Niño 4 explained the largest amount of TWSA variability in the northeastern Amazon River basin (accounting for 61 % of the variance in region B as shown in Table 2). In contrast, TNAI was the primary external forcing across central and western regions of the basin (accounting for 35 % of the variance in region A). In the northern basins of South America, including the Orinoco River basin, TNAI explained more than half of the observed variance (54 % in region C).

Combining Niño 4 and TNAI forcing terms significantly ($p < 0.05$) improved model performance for many regions within South America (Table 3 and Fig. S3), with 39 %, 66 % and 63 % of variance explained in regions A, B and C, respectively. In a given region, the combined model significantly outperformed (F test, $p < 0.05$) not only the worst of the two univariate models (in 95–100 % of the cells), but also the best one (in at least 60 % of the cells). The improvement due to the addition of Niño 4 in northern South America was higher and more widespread than that in the central and western Amazon, and higher than that due to the addition of TNAI in the northeastern Amazon.

HESSD
10, 12453–12483, 2013

Depending on the phase and amplitude of the secondary forcing index, drought or flood prone conditions may be either enhanced or damped. According to the sign of the regression coefficients (Fig. S2a and b), dry conditions in the central and western Amazon were triggered by warm SSTs either in the tropical North Atlantic or in the central Pacific (Niño 4 and TNAI were in-phase). In contrast, in the northeastern Amazon and in northern South America, dry conditions were caused by either warm central Pacific or cold tropical North Atlantic SSTs (Niño 4 and TNAI were in anti-phase).

The 2010 drought had a considerable impact on TWSAs in every region and was preceded by very large positive SST anomalies in both the Pacific and the Atlantic (Fig. 4). The 2005 drought was visible in the central and western Amazon, where it was responsible for a wide trough in the time series. The 2005 drought again was associated with positive SST anomalies in both the Pacific and the Atlantic, although their amplitudes were smaller compared to 2010. The impact of the 2011–2012 La Niñas on TWSAs may have been damped because of the considerable water deficits left after the 2010 drought.

4.2 SST lead times and TWSA relaxation times

The lead time of a given climate index was usually shorter in regions where TWSAs were dominantly forced by this index (Fig. S1). Lead times for Niño 4 were 3 months in most grid cells, except in the upper Solimões and its tributaries, and in some areas of the southern tributaries of the Solimões River, where it reached ~ 6 months. Lead times for TNAI were 3 months in the central and western Amazon, and were much longer elsewhere (from 5 months in region C to 7–8 months in region B and in the southern Amazon). The shortest lead times were generally equal to the prescribed minimum value, suggesting that predictions would improve as the prescribed minimum lead time was reduced. The impact of changing the minimum lead time within the three models is discussed in Sect. 4.4.

A shorter relaxation time τ indicates more sensitivity of the system to SST forcing and thus a shorter memory. In either the central and western Amazon or the northeast-

HESSD
10, 12453–12483, 2013

ern Amazon, mean relaxation times were shorter for the model forced by the dominant index, while they were longer for the secondary index (Fig. S2c). In northern South America, however, relaxation times were larger for the dominant index, TNAI, than for Niño 4. For the combined model, the mean relaxation time in the central and western Amazon and the northeastern Amazon was approximately one-month longer than those found by using solely the dominant index, while it took intermediate values in northern South America. Large τ values (6/12 months) were found in the downstream parts of the main rivers, floodplains and wetlands, where the land surface memory increases due to longer residence times of surface water storage and time delays associated with stream and river transport.

4.3 Seasonal variations in model performance

Each climate index had considerable month-to-month differences in their standard deviations, with annual peaks occurring in boreal fall and winter for Niño 4 and in boreal spring for TNAI (Fig. 5). Similarly, we found a clear seasonality in the monthly R^2 of our predictions (Fig. 5). The seasonal increase in R^2 was relatively larger in the central and western Amazon (approximately 50 % vs. 25 % in the other regions). In a given region, the monthly R^2 of every model had the same phase, especially for the best two models. In the central and western Amazon, the combined model was better from May to October, before and during the time terrestrial water storage reaches its lowest level (i.e. during the rainfall dry season, see Ronchail et al., 2002), with the largest R^2 values found in June and August. In the northeastern Amazon, the combined model performance was highest from January to June (i.e. during the rainfall wet season) with the largest R^2 found in March. This period spans the time when water storage recovers after the driest months and floodplain and wetlands along the Amazon main stem downstream of Manaus start to buffer excess runoff, until the maximum flooded extent is reached in May–June (see Fig. 2 of Prigent et al., 2007; Fig. 7 of Paiva et al., 2013). In northern South America, we found the highest R^2 values from March to June, during

HESSD
10, 12453–12483, 2013

and after the time water storage reached its lowest annual levels (end of dry season and beginning of wet season for rainfall).

4.4 Changes in model predictive skill with varying lead times

To study the evolution of the forecasting performance with increasing minimum lead times, we made the lower bound of the SST lead times vary from 1 to 8 months. In each region, the model trajectories usually did not cross each other (Figs. 6 and S4), so that the model ranking for any given lead time was the same than that found for the nominal 3 month minimum lead time described above, with the combined model being the best model. In the central and western Amazon, however, model 1 (Niño 4) provided better extended forecasts than model 2 (TNAI), while the opposite was true for medium- and short-range forecasts. Also, the combined model was not significantly ($p > 0.05$) better than model 1 for extended forecasts with 8 months lead times.

Overall, model performance degraded monotonically (R^2 decreased and RMSE increased) with increasing minimum lead times. In the central and western Amazon the evolution of the forecast was mainly influenced by TNAI, while in the northeastern Amazon, it was influenced by Niño 4, so that the trajectories of the combined model and the best individual index model tended to be parallel in these regions. In northern South America, both indices had important, complementary roles as predictors: Niño 4 influenced the medium- to short-range forecasts, while TNAI influenced the longer-range forecasts. As a result, in this region the combined model diverged from the other models.

In the Amazon basin, the combined model was still able to explain 31 % of the observed variance for an 8 month lead time compared to 45 % for a 1 month lead time (Fig. S4). Model degradation with increasing lead times was smaller in the northeastern Amazon (where 49 % of the variance was explained at 8 months vs. 69 % at 1 month) compared to the central and western Amazon (where 22 % of the variance was explained at 8 months vs. 43 % at 1 month). In northern South America, model degra-

HESSD
10, 12453–12483, 2013

dation was even smaller, with still 52 % of the variance explained at 8 months vs. 65 % at 1 month.

5 Discussion

5.1 Pacific and Altantic Ocean teleconnections and implications for TWSA forecasting

Complex teleconnections exist between the tropical Pacific and Atlantic ocean–atmosphere circulations. Connection between the eastern Pacific and the tropical North Atlantic is well known, with El Niño events leading to positive Atlantic SST one season (2–4 months) later (Enfield, 1996; Giannini et al., 2000; Saravanan et al., 2000). This is consistent with TNAI lagging Niño 4 by 4 months ($R > 0$) and explains the severity of the 2005 and 2010 droughts when both pools were warmer than usual (Fig. 4). On the other hand, positive SST in the TNA region trigger La Niña conditions in the central Pacific three seasons later (Ham et al., 2013), which may be the case for the 2006 and 2011 La Niñas. In terms of model structure, it suggests that the two forcing terms in the combined model are not completely independent, which may lead to a slight ambiguity in identifying the forcing source of the observed TWSA variations. In future work, spatial optimization of the forcing regions within the Pacific and Atlantic and empirical orthogonal function analysis may lead to increases in model skill and independence of the predictive information from the two ocean pools.

5.2 Model structure and uncertainties

Other studies (Chen et al., 2013a; de Linage et al., 2013) used SST as a proxy for TWSAs or other observables. Our approach was different in essence because we considered that TWSA *changes* (dTWSA/dt) were correlated with SST anomalies, or equivalently, that TWSAs were correlated with cumulative SST anomalies. This form of the equation is consistent with SST anomalies imparting precipitation–

HESSD
10, 12453–12483, 2013

evapotranspiration imbalances in South America with relatively short atmospheric transport times by means of changes in the Walker circulation or the north–south positioning of the ITCZ. We also modeled TWSA as experiencing a forced relaxation (as described by Eq. 1), thus accounting for the land surface memory. In the absence of any additional external forcing (P–E anomalies), the relaxation term causes the system to gradually return back to the mean hydrologic state. For the case of flooded conditions, this return to the mean would likely occur by means of increased drainage, runoff, and evapotranspiration. For the case of water deficit, return to the mean would occur by means of reduced plant transpiration, reduced soil evaporation, higher soil water retention (lower conductivity), and reduced surface and subsurface runoff. Use of a spatially varying relaxation term also was justified because some regions have a longer memory, for example in the Amazon downstream regions where the surface water storage component adds memory to the system, because it integrates the runoff from all the upstream regions with various delays with respect to forcing from SST anomalies.

Important next steps for reducing model uncertainties include (1) a more comprehensive evaluation of model forecasting success for time periods that were not used to calibrate model parameters as soon as more GRACE observations become available, (2) improvements to the approach for parameterization for the combined model, and (3) more detailed analysis and study of the mechanisms contributing to TWSA interannual variations in different South America regions. Improved parameterizations may include the development of new models that allow for a seasonally-varying sensitivity to the forcing, in order to increase the inter-seasonal performance of our model. To improve our understanding of the underlying mechanisms, more study is needed of the relative contributions of remote oceanic sources to the local and regional precipitation patterns (van der Ent and Savenije, 2013), as well as more detailed analysis of vegetation and deforestation controls on precipitation recycling by means of land-atmosphere couplings (Coe et al., 2009; Lee et al., 2011).

HESSD
10, 12453–12483, 2013

5.3 Potential for flood and drought forecasting in the Amazon

Floods hinder ground transportation and damage crops and infrastructure in many regions in South America. The northeastern Amazon is characterized by an extensive network of wetlands and floodplains (Prigent et al., 2007; Paiva et al., 2013) that are flooded seasonally. A strong wetting trend was observed by GRACE in these regions (Fig. 4), and may be correlated either with a decadal phase shift in the North Pacific climate linked to an equatorial Pacific surface cooling and leading to increased precipitation (de Linage et al., 2013; Kosaka and Xie, 2013) or with a warming of the Tropical North Atlantic over the last 20 yr (Gloor et al., 2013). Large hydroelectric reservoirs are also found in these regions (like the Balbina Reservoir near Manaus) that are used to generate hydroelectricity. Our 3 month combined model estimates explained a considerable amount of the variance in this region (66 % in region B) and had a level of performance higher than average during the rainfall wet season (i.e., when floodplains and wetlands are starting to fill with excess water runoff). An important next step in this context is to relate the TWSA observations and model predictions analyzed here to floodplain area, river height, and reservoir height time series using additional satellite observations (see Paiva et al., 2013).

Although floods have significant economic impacts, farmers and fishermen may be more vulnerable to droughts, because droughts hinder fluvial transportation, make crop irrigation more difficult and harm fish communities (Drapeau et al., 2011). In areas where the seasonal variation is strong, agricultural and fishery activities are conditioned by the timing of the dry and wet seasons. Early warming information about changes in this timing may be of use in reducing economic losses.

Very severe droughts like the 2005 and 2010 events may increase tree mortality in intact forests and promote understory fires that contribute to the conversion of tropical forests to savannas and croplands. Regions that are critically affected by fires include the Amazon's central and southern regions (the so-called "arc of deforestation", see Chen et al., 2013b). In these regions, the amount of soil moisture recharge during

HESSD
10, 12453–12483, 2013

the wet season critically affects transpiration, surface humidity and fires during the following dry season (Chen et al., 2013a). In the central and western Amazon our 3 month forecasts had above average seasonal performance during the rainfall dry season (May–August), thus providing additional evidence that TWSA may be another useful variable for integration into an early warning system for Amazon fires, which will eventually contribute to reducing ecosystem losses.

While SST data are available on an operational basis (1 month delay) and thus do not limit the development of forecasting models for floods or fire severity as described above, this is not the case for the GRACE-Level 2 products that are released with a 2 month minimum delay. Faster processing of the GRACE products – even with reduced quality standards – may be required for effective integration into operational forecasting systems.

6 Conclusions

We found that the spatial pattern of interannual TWSA in tropical South America was significantly controlled by variations of SST anomalies from the equatorial central Pacific and tropical North Atlantic, as represented by Niño 4 and TNAI, respectively. To predict the spatial and temporal variability of TWSA in this region, we built a series of simple statistical models.

Niño 4 was the primary external forcing for the northeastern Amazon (with 61 % of variance explained with a 3 month forecast), whereas TNAI was dominant in the central and western regions of the southern Amazon (35 % of variance explained with a 3 month forecast). Forcing the model with a combination of the two indices improved the fit significantly ($p < 0.05$) for at least two thirds of the grid cells, compared to models forced solely with Niño 4 or TNAI. The combined model was able to explain 43 % of the variance in the Amazon basin as a whole, 66 % in the northeastern regions, and 39 % in the central and western regions.

HESSD
10, 12453–12483, 2013

We studied how the forecasting skill of our combined model changed with increasing lead times from 1 to 8 months. For the Amazon basin as a whole, the model was still able to explain 31 % of the observed variance using an 8 month lead time vs. 45 % for a 1 month lead time (equivalent to a 31 % degradation). Model degradation with increasing lead times was smaller in the northeastern Amazon (up to 29 %) and larger in the central and western Amazon (up to 49 %).

These statistical models have the potential to provide early warning information about flooding in the northeastern Amazon, where floodplain areas are extensive and the sensitivity of floods to external SST forcing was high (model skill was up to 25 % higher than the annual mean during the wet season and the time of peak of flooding in this area). They also enable drought prediction, in particular in the central and western Amazon where our models had above average performance (up to 50 % higher) during the dry season. This work also strengthens our understanding of the mechanisms regulating interannual variability in Amazon fires, as TWSA deficits may subsequently lead to atmospheric water vapor deficits and more severe fire weather.

Future work will focus on validating these models against independent, more recent GRACE observations.

Supplementary material related to this article is available online at http://www.hydrol-earth-syst-sci-discuss.net/10/12453/2013/hessd-10-12453-2013-supplement.pdf.

Acknowledgements. This work was supported by the Gordon and Betty Moore Foundation (GBMF3269), NASA Atmospheric Sciences, NASA GRACE Science Team, and the Multicampus Research Programs and Initiatives of the University of California Office of the President. We thank Yang Chen for discussions on model design and Amazon hydrology.

HESSD
10, 12453–12483, 2013

References

Baker, I. T., Prihodko, L., Denning, A. S., Goulden, M., Miller, S., and da Rocha, H. R.: Seasonal drought stress in the Amazon: reconciling models and observations, J. Geophys. Res., 113, G00B01, doi:10.1029/2007JG000644, 2008.

Boening, C., Willis, J. K., Landerer, F. W., and Nerem, R. S.: The 2011 La Niña: so strong, the oceans fell, Geophys. Res. Lett., 39, L19602, doi:10.1029/2012GL053055, 2012.

Bruinsma, S., Lemoine, J.-M., Biancale, R., and Valès, N.: CNES/GRGS 10 day gravity field models (release 2) and their evaluation, Adv. Space Res., 45, 587–601, doi:10.1016/j.asr.2009.10.012, 2010.

Chen, J. L., Wilson, C. R., Tapley, B. D., Yang, Z. L., and Niu, G. Y.: The 2005 drought event in the Amazon River basin as measured by GRACE and estimated by climate models, J. Geophys. Res., 114, B05404, doi:10.1029/2008JB006056, 2009.

Chen, J. L., Wilson, C. R., and Tapley, B. D.: The 2009 exceptional Amazon flood and interannual terrestrial water storage change observed by GRACE, Water Resour. Res., 46, W12526, doi:10.1029/2010WR009383, 2010.

Chen, Y., Randerson, J. T., Morton, D. C., DeFries, R., Collatz, G. J., Kasibhatla, P. S., Giglio, L., Jin, Y., and Marlier, M. E.: Forecasting fire season severity in South America using sea surface temperature anomalies, Science, 334, 787–791, doi:10.1126/science.1209472, 2011.

Chen, Y., Velicogna, I., Famiglietti, J. S., and Randerson, J. T.: Satellite observations of terrestrial water storage provide early warning information about drought and fire season severity in the Amazon, J. Geophys. Res.-Biogeo., 118, 495–504, doi:10.1002/jgrg.20046, 2013a.

Chen, Y., Morton, D. C., Jin, Y., Gollatz, G. J., Kasibhatla, P. S., van der Werf, G. R., DeFries, R. S., and Randerson, J. T.: Long-term trends and interannual variability of forest, savanna, and agricultural fires in South America, Carbon Manage., in press, 2013b.

Chiang, J. C. H. and Vimont, D. J.: Analogous Pacific and Atlantic meridional modes of tropical atmosphere–ocean variability, J. Climate, 17, 4143–4158, 2004.

Coe, M. T., Marcos, M. H., and Soares-Filho, B. S.: The influence of historical and potential future deforestation on the stream flow of the Amazon River – land surface processes and atmospheric feedbacks, J. Hydrol., 369, 165–174, doi:10.1016/j.jhydrol.2009.02.043, 2009.

Dai, A., Qian, T., Trenberth, K. E., and Milliman, J. D.: Changes in continental freshwater discharge from 1948 to 2004, J. Climate, 22, 2773–2792, doi:10.1175/2008JCLI2592.1, 2009.

HESSD
10, 12453–12483, 2013

Davidson, E. A., de Araújo, A. C., Artaxo, P., Balch, J. K., Brown, I. F., Bustamante, M. M. C., Coe, M. T., DeFries, R. S., Keller, M., Longo, M., Munger, J. W., Schroeder, W., Soares-Filho, B. S., Souza Jr, C. M., and Wofsy, S. C.: The Amazon basin in transition, Nature, 481, 321–328, doi:10.1038/nature10717, 2012.

de Linage, C., Kim, H., Famiglietti, J. S., and Yu, J. Y.: Impact of Pacific and Atlantic sea surface temperatures on interannual and decadal variations of GRACE land water storage in tropical South America, J. Geophys. Res.-Atmos., 118, 1–19, doi:10.1002/jgrd.50820, 2013.

Dettinger, M. D., Cayan, D. R., McCabe, G. J., and Marengo, J. A.: Multiscale streamflow variability associated with El Niño/Southern Oscillation, in: El Niño and the Southern Oscillation: Multiscale Variability and Global and Regional Impacts, edited by: Diaz, H. F. and Markgraf, V., chap. 4, Cambridge University Press, Cambridge, 113–148, 2000.

Drapeau, G., Mering, C., Ronchail, J., and Filizola, N.: Variabilité hydrologique et vulnérabilité des populations du Lago Janauaca (Amazonas, Brésil), Confins, Revue franco-brésilienne de géographie/Revista franco-brasilera de geografia, 11, available at: http://confins.revues.org/6904, doi:10.4000/confins.6904 (last access: 9 October 2013), 2011.

Enfield, D. B.: Relationships of inter-American rainfall to Atlantic and Pacific SST variability, Geophys. Res. Lett., 23, 3305–3308, 1996.

Enfield, D. B., Mestas-Nuñez, A. M., Mayer, D. A., and Cid-Serrano, L.: How ubiquitous is the dipole relationship in tropical Atlantic sea surface temperatures?, J. Geophys. Res., 104, 7841–7848, 1999.

Enfield, D. B., Mestas-Nuñez, A. M., and Trimble, P. J.: The Atlantic multidecadal oscillation and its relation to rainfall and river flows in the continental US, Geophys. Res. Lett., 28, 2077–2080, 2001.

Espinoza, J. C., Ronchail, J., Guyot, J. L., Junquas, C., Vauchel, P., Lavado, W., Drapeau, G., and Pombosa, R.: Climate variability and extreme drought in the upper Solimões River (western Amazon Basin): understanding the exceptional 2010 drought, Geophys. Res. Lett., 38, L13406, doi:10.1029/2011GL047862, 2011.

Espinoza, J. C., Ronchail, J., Frappart, F., Lavado, W., Santini, W., and Guyot, J. L.: The major floods in the Amazonas River and tributaries (western Amazon basin) during the 1970–2012 period: a focus on the 2012 flood, J. Hydrometeorol., 14, 1000–1008, doi:10.1175/JHM-D-12-0100.1, 2013.

HESSD
10, 12453–12483, 2013

Frappart, F., Papa, F., da Silva, J. S., Ramillien, G., Prigent, C., Seyler, F., and Calmant, S.: Surface freshwater storage and dynamics in the Amazon basin during the 2005 exceptional drought, Environ. Res. Lett., 7, 044010, doi:10.1088/1748-9326/7/4/044010, 2012.

Giannini, A., Kushnir, Y., and Cane, M. A.: Interannual variability of Caribbean rainfall, ENSO, and the Atlantic Ocean, J. Climate, 13, 297–311, 2000.

Gloor, M., Brienen, R. J. W., Galbraith, D., Feldpausch, T. R., Schöngart, J., Guyot, J.-L., Espinoza, J. C., Lloyd, J., and Phillips, O. L.: Intensification of the Amazon hydrological cycle over the last two decades, Geophys. Res. Lett., 40, 1–5, doi:10.1002/grl.50377, 2013.

Ham, Y.-G., Kug, J.-S., Park, J.-Y., and Jin, F.-F.: Sea surface temperature in the north tropical Atlantic as a trigger for El Niño/Southern Oscillation events, Nat. Geosci., 6, 112–116, doi:10.1038/NGEO1686, 2013.

Kosaka, Y. and Xie, S.-P.: Recent global-warming hiatus tied to equatorial Pacific surface cooling, Nature, 501, 403–407, doi:10.1038/nature12534, 2013.

Kitoh, A., Endo, H., Krishna Kumar, K., Cavalcanti, I. F. A., Goswami, P., and Zhou, T.: Monsoons in a changing world: a regional perspective in a global context, J. Geophys. Res.-Atmos., 118, 3053–3065, doi:10.1002/jgrd.50258, 2013.

Lee, J.-E., Lintner, B. R., Boyce, C. K., and Lawrence, P. J.: Land use change exacerbates tropical South American drought by sea surface temperature variability, Geophys. Res. Lett., 38, L19706, doi:10.1029/2011GL049066, 2011.

Lewis, S. L., Brando, P. M., Phillips, O.L., van der Heijden, G. M. F., and Nepstad, D.: The 2010 Amazon drought, Science, 331, 554, 2011.

Liebmann, B. and Marengo, J. A.: Interannual variability of the rainy season and rainfall in the Brazilian Amazon basin, J. Climate, 14, 4308–4318, doi:10.1002/joc.815, 2001.

Lima, C. H. R. and Lall, U.: Climate informed monthly streamflow forecasts for the Brazilian hydropower network using a periodic ridge regression model, J. Hydrol., 380, 438–449, doi:10.1016/j.jhydrol.2009.11.016, 2010.

Marengo, J. A., Nobre, C. A., Tomasella, J., Oyama, M. D., Sampaio de Oliveira, G., de Oliveira, R., Camargo, H., Alves, L. M., and Brown, I. F.: The drought of Amazonia in 2005, J. Climate, 21, 495–516, doi:10.1175/2007JCLI1600.1, 2008.

Marengo, J. A., Tomasella, J., Alves, L. M., Soares, W. R., and Rodriguez, D. A.: The drought of 2010 in the context of historical droughts in the Amazon region, Geophys. Res. Lett., 38, L12703, doi:10.1029/2011GL047436, 2011.

HESSD
10, 12453–12483, 2013

McCabe, G. J., Palecki, M. A., and Betancourt, J. L.: Pacific and Atlantic Ocean influences on multidecadal drought frequency in the United States, P. Natl. Acad. Sci. USA, 101, 4136–4141, doi:10.1073/pnas.0306738101, 2004.

Miller, S. D., Goulden, M. L., Hutyra, L. R., Keller, M., Saleska, S. R., Wofsy, S. C., Figueira, A. M. S., da Rocha, H. R., and de Camargo, P. B.: Reduced impact logging minimally alters tropical rainforest carbon and energy exchange, P. Natl Acad. Sci. USA, 108, 19431–19435, doi:10.1073/pnas.1105068108, 2011.

Molinier, M., Ronchail, J., Guyot, J.-L., Cochonneau, G., Guimarães, V., and de Oliveira, E.: Hydrological variability in the Amazon drainage basin and African tropical basins, Hydrol. Process., 23, 3245–3252, doi:10.1002/hyp.7400, 2009.

Paiva, R. C. D., Buarque, D. C., Collischonn, W., Bonnet, M.-P., Frappart, F., Calmant, S., and Mendes, C. A. B.: Largescale hydrologic and hydrodynamic modeling of the Amazon River basin, Water Resour. Res., 49, 1226–1243, doi:10.1002/wrcr.20067, 2013.

Phillips, O. L. Aragão, L. E. O. C., Lewis, S. L., Fisher, Joshua B., Lloyd, J., López-González, G., Malhi, Y., Monteagudo, A., Peacock, J., Quesada, C. A., van der Heijden, G., Almeida, S., Amaral, I., Arroyo, L., Aymard, G., Baker, T. R., Bánki, O., Blanc, L., Bonal, D., Brando, P., Chave, J., Alves de Oliveira, A. C., Dávila Cardozo, N., Czimczik, C. I., Feldpausch, T. R., Aparecida Freitas, M., Gloor, E., Higuchi, N., Jiménez, E., Lloyd, G., Meir, P., Mendoza, C., Morel, A., Neill, D. A., Nepstad, D.,Patiño, S., Peñuela, M. C., Prieto, A., Ramírez, F., Schwarz, M., Silva, J., Silveira, M., Thomas, A. S., ter Steege, H., Stropp, J., Vásquez, R., Zelazowski, P., Alvarez Dávila, E., Andelman,S., Andrade,A.,Chao, K.-J., Erwin, T., Di Fiore, A., Honorio C., E., Keeling, E., Killeen, T. J., Laurance, W. F., Peña Cruz, A., Pitman, N. C. A., Núñez Vargas, P., Ramírez-Angulo, H., Rudas, A., Salamão, R., Silva, N., Terborgh, J., and Torres-Lezama, A.: Drought sensitivity of the Amazon rainforest, Science, 323, 1344–1347, doi:10.1126/science.1164033, 2009.

Prigent, C., Papa, F., Aires, F., Rossow, W. B., and Matthews, E.: Global inundation dynamics inferred from multiple satellite observations, 1993–2000, J. Geophys. Res., 112, D12107, doi:10.1029/2006JD007847, 2007.

Reager, J. T. and Famiglietti, J. S.: Global terrestrial water storage capacity and flood potential using GRACE, Geophys. Res. Lett., 36, L23402, doi:10.1029/2009GL040826, 2009.

Richey, J. E., Nobre, C., and Deser, C.: Amazon river discharge and climate variability: 1903 to 1985, Science, 246, 101–103, 1989.

HESSD
10, 12453–12483, 2013

Richey, J. E., Melack, J. M., Aufdenkampe, A. K., Ballester, V. M., and Hess, L. L.: Outgassing from Amazonian rivers and wetlands as a large tropical source of atmospheric CO_2, Nature, 416, 617–620, 2002.

Ronchail, J., Cochonneau, G., Molinier, M., Guyot, J.-L., de Miranda Chaves, A., Guimarães, V., and de Oliveira, E.: Interannual rainfall variability in the Amazon basin and sea-surface temperatures in the equatorial Pacific and the tropical Atlantic oceans, Int. J. Climatol., 22, 1663–1686, doi:10.1002/joc.815, 2002.

Ropelewski, C. F. and Hapert, M. S.: Global and regional scale precipitation patterns associated with the El Niño/Southern Oscillation, Mon. Weather Rev., 115, 1606–1626, 1987.

Saravanan, R. and Chang, P.: Interaction between tropical Atlantic variability and El Niño-Southern Oscillation, J. Climate, 13, 2177–2194, 2000.

van der Ent, R. J. and Savenije, H. H. G.: Oceanic sources of continental precipitation and the correlation with sea surface temperature, Water Resour. Res., 49, 3993–4004, doi:10.1002/wrcr.20296, 2013.

Yoon, J.-H. and Zeng, N.: An Atlantic influence on Amazon rainfall, J. Climate, 34, 249–264, doi:10.1007/s00382-009-0551-6, 2010.

Zeng, N.: Seasonal cycle and interannual variability in the Amazon hydrologic cycle, J. Geophys. Res., 104, 9097–9106, 1999.

Zeng, N., Yoon, J.-H., Marengo, J. A., Subramaniam, A., Nobre, C. A., Mariotti, A., and Neelin, J. D.: Causes and impacts of the 2005 Amazon drought, Environ. Res. Lett., 3, 014002, doi:10.1088/1748-9326/3/1/014002, 2008.

HESSD
10, 12453–12483, 2013

Table 1. Description of the 3 models: parameters, predictor variables, degrees of freedom, and number of variables.

Model #	Forcing term ($F(t)$ in Eq. 1)*	DOF	Number of variables
1	$\boldsymbol{a}_0(x) \cdot$ Niño 4 $(t - \boldsymbol{\alpha}(x))$	3	1
2	$\boldsymbol{b}_0(x) \cdot$ TNAI $(t - \boldsymbol{\beta}(x))$	3	1
3	$\boldsymbol{a}_0(x) \cdot$ Niño 4 $(t - \boldsymbol{\alpha}(x)) + \boldsymbol{b}_0(x) \cdot$ TNAI $(t - \boldsymbol{\beta}(x))$	4	2

* Model parameters are highlighted in bold.

HESSD
10, 12453–12483, 2013

Table 2. Statistics of models performance averaged within each region delineated in Fig. 1. Every model fit is significant (F test, $p < 0.05$) within at least 90 % of the cells in each region.

Model #	R^2				RMSE (mm)/NRMSE (%)			
	Amazon basin	Region A	Region B	Region C	Amazon basin	Region A	Region B	Region C
1	0.35	0.23	0.61	0.36	50/81	50/89	65/62	48/81
2	0.28	0.35	0.25	0.54	55/85	45/80	91/86	41/68
3	0.43	0.39	0.66	0.63	46/75	44/78	61/58	36/61

HESSD
10, 12453–12483, 2013

Table 3. Statistical comparison between different models pairs using an F test ($p < 0.05$). See Fig. S3 for the distributed F values.

Models pair	DOF difference	$F_{0.05}$	% cells with significant F ($F > F_{0.05}$)				Mean F			
			Amazon basin	Region A	Region B	Region C	Amazon basin	Region A	Region B	Region C
(1,3)	1	3.9	64	95	83	100	31	39	20	90
(2,3)	1	3.9	75	60	100	79	59	11	145	40

HESSD
10, 12453–12483, 2013

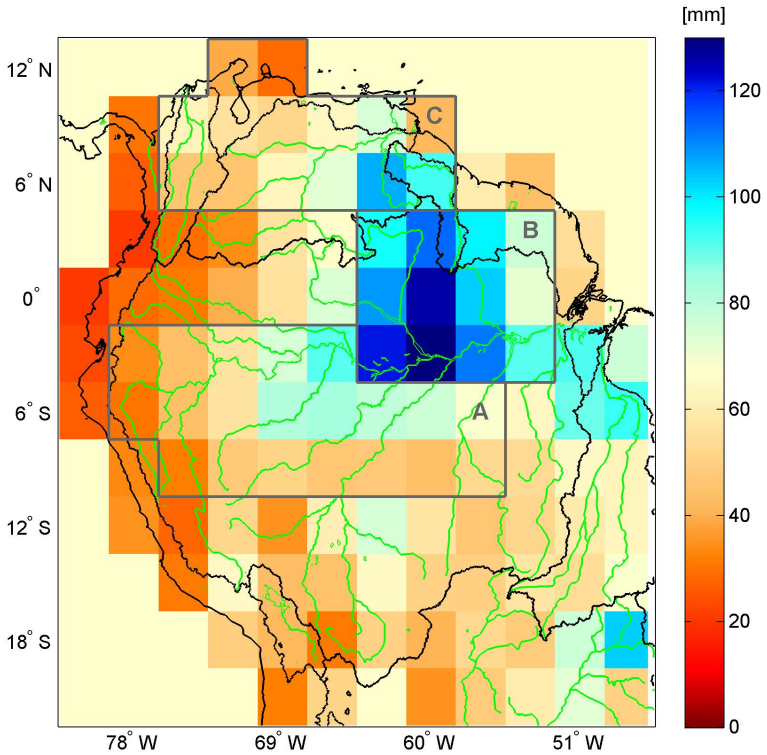

Fig. 1. Standard deviation of terrestrial water storage anomalies (TWSAs) interannual variations as observed by GRACE for August 2002 to July 2012. A, B and C indicate regions that were used to compute the TWSA time series plotted in Fig. 5. A climatological mean annual cycle of monthly means was removed from the TWSA time series prior to computing the standard deviation of the interannual variations. Contours of the main watersheds are plotted in black and the main rivers and their tributaries are plotted in green.

HESSD
10, 12453–12483, 2013

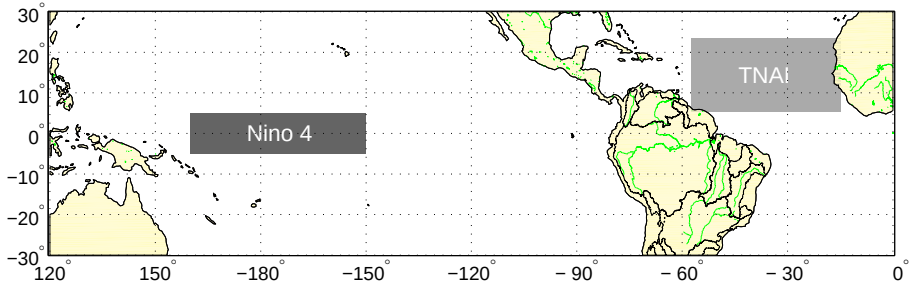

Fig. 2. The central Pacific (Niño 4) and the tropical North Atlantic index (TNAI) regions (shaded gray areas) whose average temperatures anomalies are correlated with interannual terrestrial water storage changes in tropical South America.

HESSD
10, 12453–12483, 2013

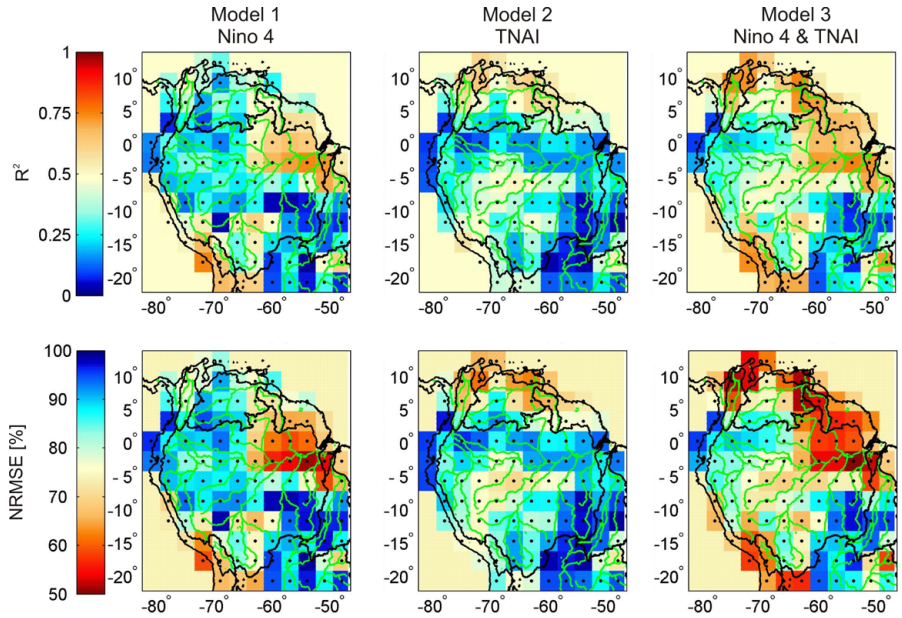

Fig. 3. Coefficient of determination (R^2) and normalized root mean square error (NRMSE) for the three models described in Table 1 and computed for the period from August 2002 through July 2012. The RMSE was normalized at each location using the standard deviation of GRACE interannual terrestrial water storage anomalies shown in Fig. 1. The prescribed minimum lead time for the three models was 3 months. Cells where the linear fit was significant ($p < 0.05$) are marked with a black dot.

HESSD
10, 12453–12483, 2013

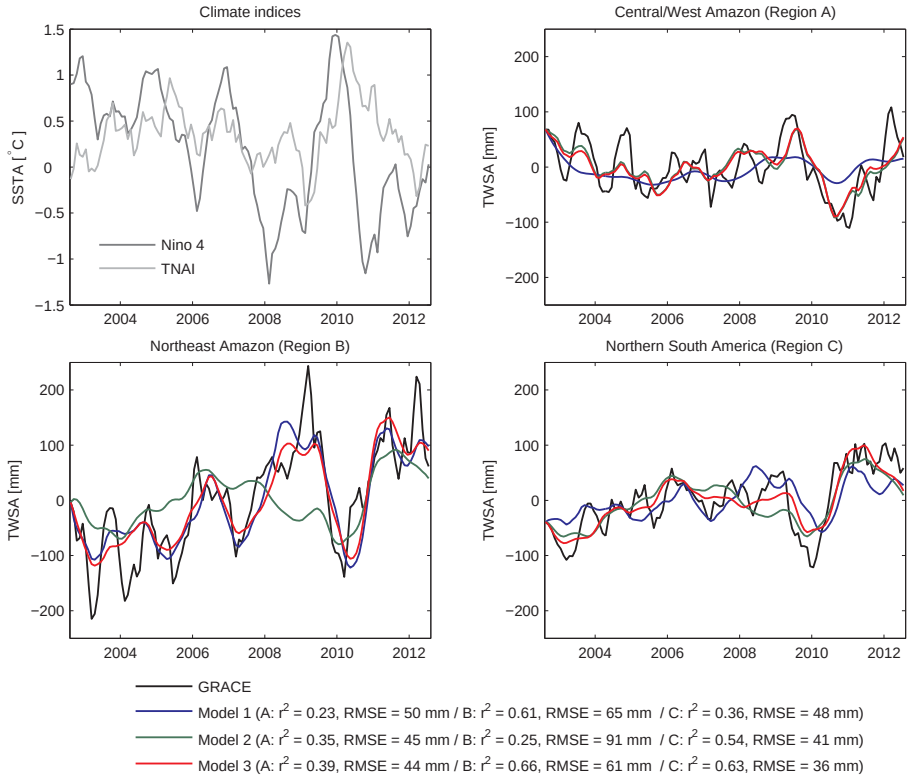

Fig. 4. Top left subplot: the monthly Niño 4 index (dark gray line) and the Tropical North Atlantic Index (light gray line). Top right and bottom subplots: GRACE-observed (black line) and model-predicted TWSAs for each of the three regions delineated in Fig. 1, for the three models described in Table 1. Regional averages of model performances (Table 2) are also provided for each model. The prescribed minimum lead time between SST indices and TWSAs was equal to 3 months.

HESSD
10, 12453–12483, 2013

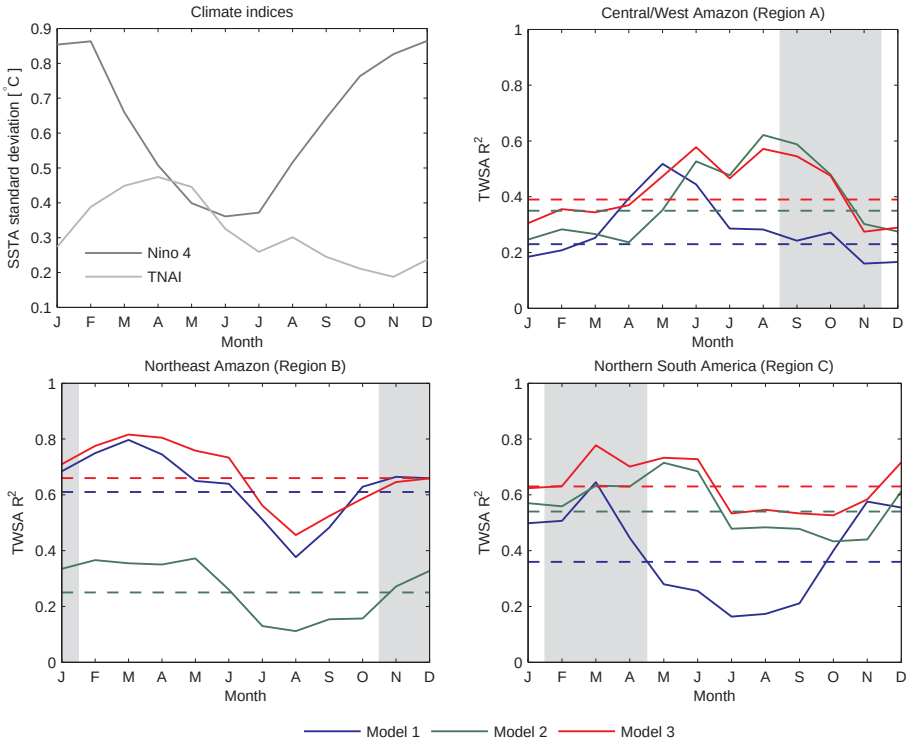

Fig. 5. Top left subplot: monthly climatology of the standard deviation of SST-based climate indices with no lag applied. Top right and bottom subplots: monthly climatology of R^2 between observed and predicted TWSAs averaged over each of the three regions delineated in Fig. 1, for the three models described in Table 1 (with a 3 month prescribed minimum lead time). Dashed lines represent the R^2 computed for all months. The gray shaded areas represent the three driest months in a year, computed from the GRACE TWSA mean monthly climatology.

HESSD
10, 12453–12483, 2013

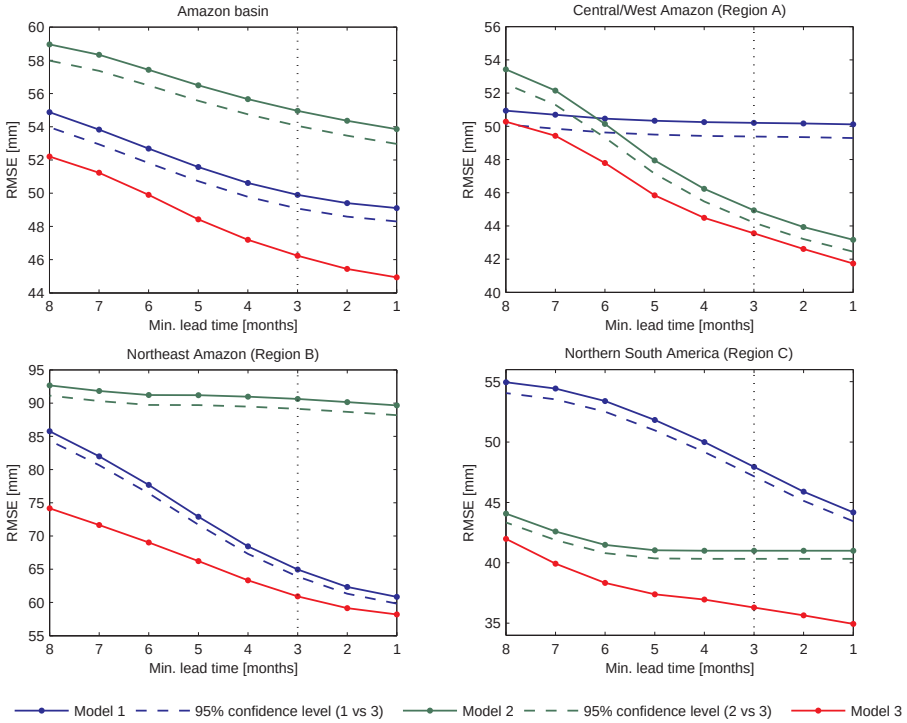

Fig. 6. RMSE vs. prescribed minimum SST lead time for the three models, averaged over each of the three regions delineated in Fig. 1. Dashed lines bound the 95 % confidence intervals within which the models either forced by Niño 4 (model 1) or TNAI (model 2) are statistically different from the combined model (model 3). The vertical dotted line represents the minimum lead time that was used in the previous figures. Results for R^2 are shown in Fig. S4.

HESSD
10, 12453–12483, 2013

Forecasting terrestrial water storage changes in the Amazon Basin

C. de Linage et al.